Journal of Industrial and Engineering Chemistry 146 (2025) 788–799

Contents lists available at ScienceDirect

Journal of Industrial and Engineering Chemistry

journal homepage: www.elsevier.com/locate/jiec

Thermophysical Characterization of Sustainable Pathways for Hydrofluorocarbons Separation Utilizing Deep Eutectic Solvents

L.V.T.D. Alencar [a,b], B. González-Barramuño [c], S.B. Rodriguez-Reartes [a,d,e], H. Quinteros-Lama [f], J.M. Garrido [c], V. Codera [h], J.O. Pou [h], F.W. Tavares [b,g], R. Gonzalez-Olmos [h], F. Llovell [a,*]

[a] Department of Chemical Engineering, ETSEQ, Universitat Rovira i Virgili, Avinguda Països Catalans 26, 43007 Tarragona, Spain
[b] Programa de Engenharia Química (PEQ/COPPE), Universidade Federal do Rio de Janeiro (UFRJ), Athos da Silveira Ramos avenue, 149 - Block G -Ilha do Fundão, Rio de Janeiro, RJ, Brazil
[c] Departamento de Ingeniería Química, Universidad de Concepción, Concepción 4070386, Chile
[d] Departamento de Ingeniería Química, Universidad Nacional del Sur (UNS), Avda. Alem 1253, Bahía Blanca 8000, Argentina
[e] Planta Piloto de Ingeniería Química – PLAPIQUI (UNS-CONICET), Camino "La Carrindanga" Km 7, Bahía Blanca 8000, Argentina
[f] Departamento de Tecnologías Industriales, Universidad de Talca, Merced 437, Curicó, Chile
[g] Engenharia de Processos Químicos e Bioquímicos, Escola de Química (EPQB), Universidade Federal do Rio de Janeiro (UFRJ), Athos da Silveira Ramos Avenue, 149 - Block E - Ilha do Fundão, Rio de Janeiro, RJ, Brazil
[h] IQS School of Engineering, Universitat Ramon Llull, Via Augusta 390 08017 Barcelona, Spain

ARTICLE INFO

Keywords:
Hydrofluorocarbons
Refrigeration
Deep Eutectic Solvents
Solubility
soft-SAFT

ABSTRACT

The widespread use of hydrofluorocarbons (HFCs) in refrigeration ushered in a significant environmental challenge due to their high global warming potential. Effective recovery and separation techniques are imperative to mitigate their adverse impacts and promote sustainability. This study investigates the solubility behavior of four common HFCs (R-125, R-134a, R-32, and R143a) using choline chloride ([Ch]Cl) and tetramethylammonium chloride (TMAC) based Deep Eutectic Solvents (DESs) as ecofriendly, low-toxicity and low-cost alternatives, provided the promising selectivity exhibited by some of them in separating HFC mixtures. The new experimental data are completed by a comprehensive thermodynamic characterization employing the soft-SAFT equation. This modeling enables the description of the density and viscosity of pure DESs, enthalpy and entropy of dissolution, Henry's constants, and ideal selectivity. From these results, the competitive selectivity among gases in multi-component blends and DESs is predicted. R-32 appears to have the highest affinity in DESs, followed by R-134a, R-143a, and R-125, while TMAC:EG (1:3) shows the highest absorption capacity for all HFCs. Despite relatively low absorption rates, DESs containing TMAC:GL (1:3) and [Ch]Cl:GL (1:3) + 10 wt% exhibit promising selectivity for separating HFCs mixtures, especially those containing R-32, which holds significance for applications in recovering commercial blends like R410A and R407F.

Introduction

Currently, global warming represents one of the most pressing topics in modern science, exerting far-reaching impacts across virtually all areas of society, and serving as an incentive for public policies, regulations, and studies [1]. The advance of this phenomenon can be attributed mainly to the anthropogenic emission of greenhouse gases (GHGs), whose atmospheric concentration has increased in recent years [2]. Historically, the most common GHGs have been carbon dioxide, nitrous oxide, methane, and fluorinated gases (F-gases), mostly hydrofluorocarbons (HFCs) [3]. The latter are famously employed as replacements for chlorofluorocarbons and hydrochlorofluorocarbons, phased out in the Montreal Protocol in 1987 after demonstrating their ozone-depleting potential [4].

F-gases are mainly employed in the refrigeration industry and are emitted at much lower rates than other GHGs. As of 2019, these compounds accounted for approximately 2.3 % of the total GHG emissions globally [5]. However, their high global warming potential (GWP), usually thousands of times the value of CO_2, dramatically raises their impact, leading to further regulations to lessen global warming effects. The Kigali Amendment to the Montreal Protocol [6] established the future of usage of F-gases, aiming to significantly decrease global

* Corresponding author.
E-mail address: felix.llovell@urv.cat (F. Llovell).

https://doi.org/10.1016/j.jiec.2024.12.005
Received 10 July 2024; Received in revised form 15 October 2024; Accepted 2 December 2024
Available online 5 December 2024

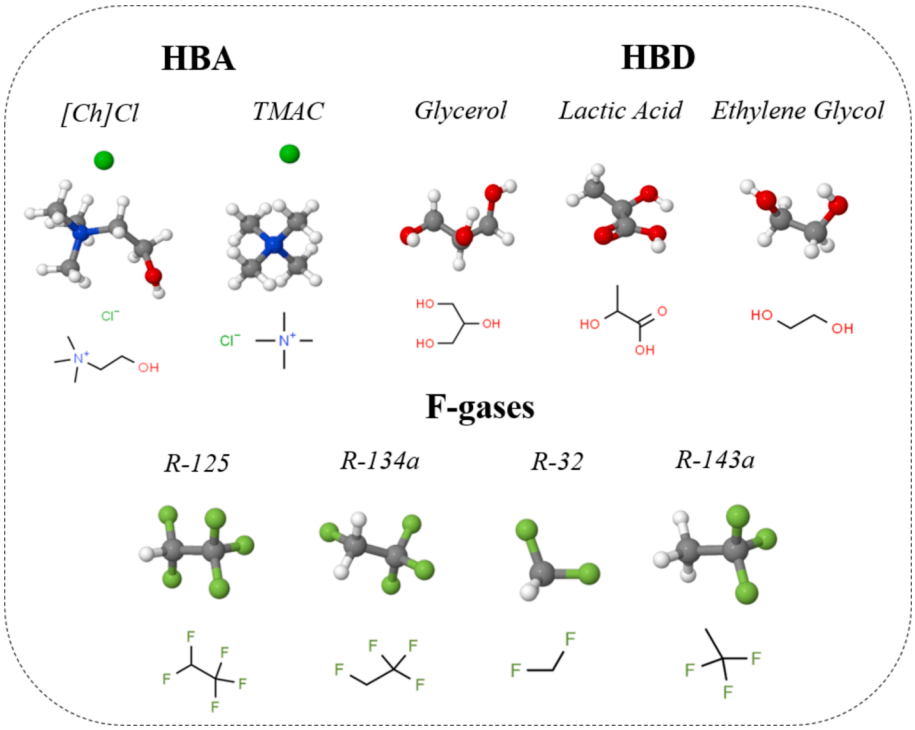

Fig. 1. Chemical structures of the compounds studied in this work.

hydrofluorocarbon emissions to 0.9–1 Gt of CO_2 equivalent per year by 2050, along with a reduction in the surface warming to 0.04 °C by 2100, which presents an encouraging contrast to current projections of 1.9–3.6 Gt of CO_2 equivalent per year and surface warming of 0.14–0.31 °C, respectively [7]. Nonetheless, there are several challenges to address. For example, it is essential to determine the source of emissions and analyze the appropriate methods for reducing them from specific sources [8]. The emissions of HFCs, in particular, have shown a significant increase over time [7,9]. Thus, treating these substances represents one of the most challenging tasks in modern chemical engineering.

Destruction of HFCs is the most direct approach to remove these compounds. However, it still copes with difficulties such as high energy demands, hazardous decomposition products under non-optimal conditions, and lack of technological availability in every country [10,11]. A circular economy framework around F-gases may circumvent this issue, reducing the requirement to produce new HFCs [11]. Regardless of the approach, an efficient and highly selective recovery of these gases from end-of-life equipment is crucial for adhering to mid and long-term phase-out regulations. However, the presence of HFCs in highly non-ideal conditions, such as azeotropic blends [12], limits the alternatives to perform such a separation process.

Among techniques involved in recovering HFCs, absorption into ionic liquids (ILs) and deep eutectic solvents (DESs) has raised as a promising alternative. The application of ILs to the absorption process is widely spread in the literature [13–16], while DESs have been studied in a more limited way, with a significant increase over the past years [17,18]. DESs are liquid mixtures that develop a solid–liquid transition at much lower temperatures than the ones of their independent components. The main driving force behind this phenomenon is attributed to hydrogen bond occurrence between both components in the DES, the hydrogen-bond acceptor (HBA) and the hydrogen-bond donor (HBD). A great number of combinations between different HBAs and HBDs may be defined, along with the molar ratio of each one. Similar to ILs, various combinations of these compounds result in DESs that exhibit varying interactions with different solutes, allowing the tunability of solvents to enhance selectivity towards specific HFCs. Moreover, some advantages have been attributed to DESs over ILs, namely lower toxicity, viscosity, and corrosivity, better degradability and lower production cost [18].

The large number of possible HBA-HBD combinations to synthesize DESs makes a complete experimental characterization challenging to achieve. Aiming to tackle this problem, computational modeling approaches have been explored in recent years. In particular, machine learning techniques have emerged as a promising approach for predicting DESs properties [19–22] and for designing task-specific DESs [23]. These models enable rapid screening of potential DES candidates, significantly reducing the need for extensive experimental work. However, careful attention is required to ensure that the models obtained through machine learning can be reliably extrapolated. Regarding the analysis of DESs and their absorption capabilities for fluids, molecular simulation and *ab initio* methods have been widely employed [24–29], providing remarkably detailed information regarding their microscopic behavior and its extension to macroscopic observables. However, the associated computational cost hinders the chance of screening for interesting DES-solute combinations, especially when considering the variety of mixtures of solutes and/or different operating conditions for the absorption process.

Merging a remarkable predictive capability with a lower computational cost, molecular-based Equations of State (EoS), such as the Statistical Associating Fluid Theory (SAFT), [30,31] have shown remarkable efficacy in precisely describing thermodynamic properties of HFCs. This framework becomes a compelling tool for the systematic design of refrigerant blends [32–37]. Their success stems from their ability to explicitly consider micro-level characteristics, such as molecular structure and intermolecular interactions, following a coarse-grained methodology, thereby elucidating their influence on observable macro-level phenomena. Previous studies have highlighted the accuracy and predictive power of the soft-SAFT EoS variant [38] in characterizing the thermodynamic behavior of HFCs [39–41], including the modeling of their solubility in DESs [42,43].

This work is devoted to verifying the absorption potential of four common HFCs (R-125, R-134a, R-32, and R143a) using specific low-cost, non-toxic, and environmentally friendly DESs. For this purpose, novel experimental measurements on the solubility of those gases in DESs composed of tetramethylammonium chloride (TMAC) as hydrogen

bond acceptor (HBA), combined with ethylene glycol and glycerol as hydrogen bond donors (HBD), are presented here. These data, along with some recently published data for choline chloride ([Ch]Cl) based DESs with the same HBDs and lactic acid [44,45], are accurately characterized using the soft-SAFT EoS. [Ch]Cl and TMAC-based systems, classified as type III DESs, are widely used, readily available, and cost-effective solvents [46]. Furthermore, [Ch]Cl-based DESs have previously demonstrated promising selectivity values for blends comprised of HFCs, placing them as interesting solvents for the design and evaluation of new recovery processes [44,45]. These solvents are also characterized by the possibility of tuning their selectivity towards different HFC combinations by the choice of specific HBDs. TMAC-based DESs have been included to get a more complete picture of the capabilities of type III DESs for F-gases separation. Fig. 1 illustrates the molecular structures of all compounds studied in this work.

The thermophysical model is then used to describe various properties, including the density and viscosity of pure DESs, the enthalpy and entropy of dissolution, Henry's constants, and ideal selectivity. The study additionally predicts the competitive selectivity among gases in multi-component mixtures based on commercial refrigerant blends and DESs. Based on this information, a rational analysis is conducted to determine the best DES for the recovery of specific components in commercial refrigerant systems, facilitating the pre-design of a gas separation unit for industrial applications.

Materials and methods

Materials

Glycerol (99 % purity) and ethylene glycol (99 % purity) were acquired from ITW Reagents. Tetramethylammonium chloride (97 % purity) was purchased from Thermo Fischer Scientific, and it was heated at 343.15 K under vacuum conditions for 15 h for further purification. The hydrofluorocarbons utilized in all experiments were R134a, R-125, R-32, and R-143a, all sourced from GRIT, Gases, Research, Innovation & Technology S.L.U, with a purity level of at least 99.5 %.

The DESs experimentally characterized in this study were prepared following the methodology used by Codera et al. [44]. In particular, the HBA tetramethylammonium chloride (TMAC) was combined with glycerol (GL) or ethylene glycol (EG) in a molar ratio of 1:3. During the preparation of DESs, [Ch]Cl and TMAC HBAs were placed in a vacuum oven at 343.15 K before use. After the drying process, they were stored in a drying system containing phosphorus pentoxide to avoid any further hydration. The standard procedure established by Moradi et al. [47] and Nkosi et al. [48] was followed in all cases. DESs were prepared in a beaker using a Mettler Toledo PM2000 balance with an uncertainty of ± 0.01 g and heated at 338.15 K for 1 h with continuous stirring until a uniform, transparent liquid was formed. The beaker was sealed during the DES preparation. In the particular case of the aqueous [Ch]Cl: GL (1:3) system, water was added to the DES and controlled gravimetrically, until obtaining a 10 wt% of water content.

Methods

Determination of DESs density and viscosity

The density and viscosity of DESs were measured using a digital densimeter and viscometer over a temperature range of 293.15 to 343.15 K, in 5 K increments, under atmospheric pressure. Two measurements were performed for each DES and property, and the results are expressed as the average, with a measurement uncertainty of 0.0001 $g \cdot cm^{-3}$ for density and ± 0.1 mPa·s for viscosity.

Detailed information regarding the experimental equipment and setup for density and viscosity measurements can be found in previous work [44] and in section S1 of the Supporting Information.

Determination of hydrofluorocarbons solubility

HFC solubility was determined using an isochoric saturation analytical method with a custom-built apparatus. A known amount of DES (± 0.01 g) was introduced into the equilibrium cell, and the entire system was evacuated for 2 h at 300.15 K using a vacuum pump (COMECTA − IVYMEN, model 5900621). Meanwhile, HFC from the commercial bottle was introduced into the gas cylinder of the system, with the temperature set at 300.15 K. Once equilibrium was reached, the vacuum was stopped, and the gas from the cylinder was swiftly transferred into the cell while stirring, causing an initial pressure increase. The system was maintained at 300.15 K, digitally recording the pressure inside the equilibrium cell every second until complete absorption occurred, evidenced by a stable equilibrium pressure persisting for at least 30 min. The uncertainty of gas solubility measurements on a mole fraction basis was determined to be ± 0.0005. Further details of the experimental method and uncertainties of gas solubilities measurements, including the necessary equations for solubility calculations, can be found in section S1 and Table S1 of the Supporting Information section.

Thermophysical modeling methodology

The thermophysical analysis of the absorption of refrigerants in DESs involves the application of two complementary approaches. First, thermodynamic modeling, necessary to build a model for each molecule and estimate the main thermodynamic properties, is done through the soft-SAFT equation of state (EoS), a well-known variant of the original Statistical Associating Fluid Theory (SAFT) approach [30,31]. The theoretical fundamentals of both approaches are explained in section S2 of the Supporting Information section.

The thermodynamic modeling of pure fluids using soft-SAFT EoS requires determining a set of molecular parameters that describe the main structural and energetic characteristics of the compounds. The molecular models used with soft-SAFT to describe DESs are a key aspect during the parameterization of molecular parameters and their future transferability. In this regard, in this work DESs are modeled as a mixture of two independent species, using the individual component approach [49], where a specific molecular model for each compound

Table 1
Molecular weight and soft-SAFT molecular parameters optimized for the species that form DESs, water, and HFCs studied in this work.

Compound	M_w (g/mol)	m	σ(Å)	ε/k_B(K)	ε^{HB}/k_B(K)	k^{HB}(Å^3)	N. of sites	Ref.
[Ch]Cl	139.63	5.096	3.401	428.4	3384	2100	1 + 1	[49]
TMAC	109.6	3.818	3.413	360.8	3384	2100	1 + 1	[50]
Glycerol	92.09	2.397	3.638	392.95	4945	2250	1 + 1	[51]
Lactic Acid	90.08	1.812	4.059	433.1	1510	3200	1 + 1	[50]
Ethylene glycol	62.07	1.751	3.668	326.05	4384	4195	1 + 1	[52]
Water	18.02	1.000	3.154	365.0	2388	2932	2 + 2	[53]
R-125	120.02	1.392	4.242	148.8	1685	24,050	1 + 1	[54]
R-134a	102.03	1.392	4.166	166.6	1862	24,050	1 + 1	[37]
R-143a	84.04	1.392	4.103	149.0	1717	24,050	1 + 1	[35]
R-32	52.00	1.321	3.529	144.4	1708	24,050	1 + 1	[54]

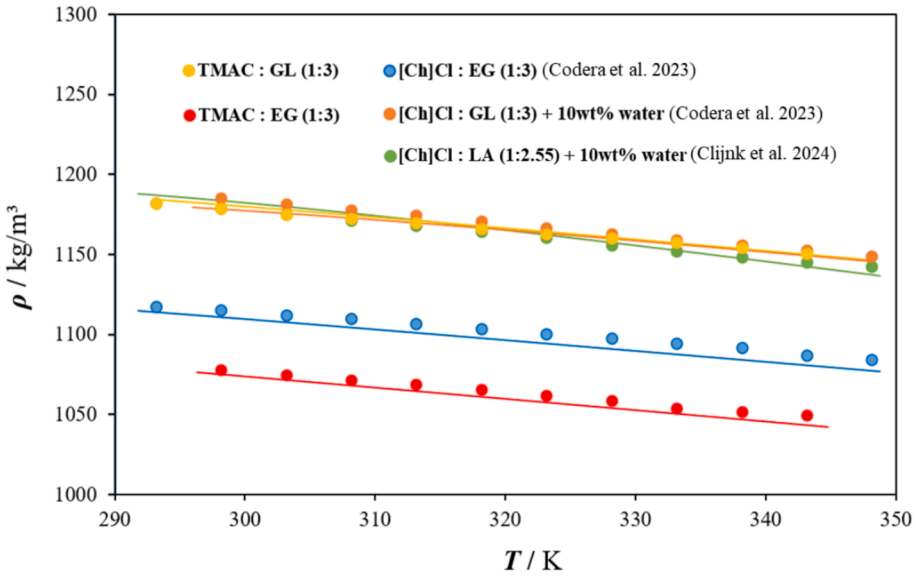

Fig. 2. Density (ρ) – temperature (T) diagram, at atmospheric pressure, for the DESs: TMAC:EG (1:3), TMAC:GL (1:3), [Ch]Cl:LA (1:2.55) + 10 wt% water, [Ch]Cl:GL (1:3) + 10 wt% water and [Ch]Cl:EG (1:3). Symbols correspond to experimental results of this work and literature data [44,45] and lines to soft-SAFT modelling (with parameters from Table 1).

comprising the investigated DESs is required. Two HBAs ([Ch]Cl and TMAC) and three HBDs (ethylene glycol – EG, glycerol – GL, and lactic acid – LA), forming a total of 5 combinations (the combination between TMAC and LA was not studied), were examined in detail. Following previous works [49,50], [Ch]Cl and TMAC are modeled as associating compounds with two association sites each, one positive and one negative, simulating the cation–anion interaction. GL, LA, and EG are also modeled with two association sites, one positive and one negative, to mimic the hydroxyl groups present in these molecules, following the same hypothesis of previous works [50–52]. Since some DESs contain water, such as the [Ch]Cl: GL (1:3) system with the addition of 10 wt% water to reduce viscosity [44], and the [Ch]Cl: LA (1:2.55) system, where the LA used had a declared purity of 85 wt% [45] (meaning the DES contains approximately 10 wt% water as an impurity), it is crucial to consider the impact of this water content on the properties of the mixture. Consequently, water is modeled using four association sites, as proposed by Vega et al. [53], to preserve the tetrahedral structure of the molecule when hydrogen bonding occurs.

Finally, all HFCs, R-125, R-134a, R-143a, and R-32, are described as homonuclear chains with two association sites each, one positive and one negative, simulating the dipole moment caused by the electronegativity of the molecule. This model has shown the best performance when describing interactions with ILs and DESs [42,43].

The complete set of parameters for all compounds is taken from previous works [35,37,49–54] and is presented in Table 1 for completeness.

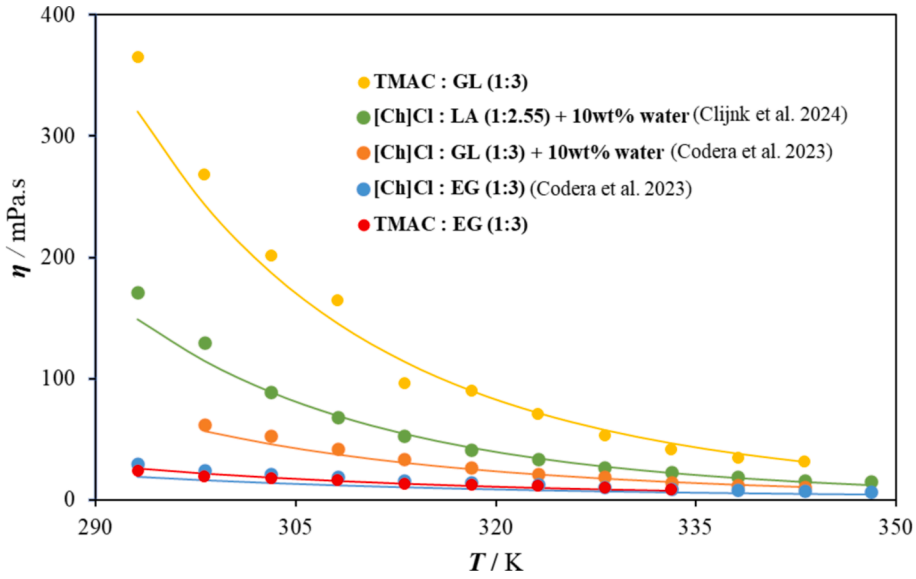

Fig. 3. Viscosity (η) – temperature (T) diagram, at atmospheric pressure for the DESs: TMAC:EG (1:3), TMAC:GL (1:3), [Ch]Cl:LA (1:2.55) + 10 wt% water, [Ch]Cl: GL (1:3) + 10 wt% water and [Ch]Cl:EG (1:3). Symbols correspond to experimental results of this work and literature data [44,45], while the lines to soft-SAFT + FVT calculations.

Table 2
Free-Volume Theory viscosity parameters optimized for DESs forming molecules.

Compound	α(J m^3 mol^{-1} kg^{-1})	B·10^2	L_v·10^2(Å)	Ref.
[Ch]Cl	374.58	0.6867	0.0170	[49]
GL	335.74	0.2794	2.9452	[49]
Water	485.21	0.1001	1.4239	[49]
EG	356.55	0.0911	8.5466	[49]
LA	449.05	0.0639	1.3881	*This work*
TMAC	379.55	0.7920	0.0042	*This work*

Results and Discussion

Solvents thermophysical characterization

Density

The new experimental density measurements performed for TMAC with EG and GL at a molar ratio 1:3 are provided in Table S3 of the Supporting Information. These measurements, along with density data from three additional DESs based on [Ch]Cl and EG, GL + 10 wt% water, and LA + 10 wt% water [44,45], are illustrated in Fig. 2 for visual analysis.

As observed, the density exhibits a consistent linear decrease with temperature in all cases, as reported in previous studies [44,55,56]. Among the evaluated DESs systems, [Ch]Cl:GL (1:3) with 10 wt% water content displays the highest density, although very closely followed by TMAC:GL (1:3) and [Ch]CL:LA (1:2.55) with 10 wt% water content. However, the DESs formed with EG have lower densities, with TMAC:EG (1:3) providing the lowest values. This trend underscores the influence of the DESs component characteristics on density variations, mostly related to molecular size. In this regard, it can be noticed that the choice of the HBD has a major impact, as DESs containing GL ([Ch]Cl:GL + 10 wt% water and TMAC:GL) and LA ([Ch]Cl:LA + 10 wt% water) exhibit higher densities, attributed to their larger molecular sizes (see Table 1 and Fig. 1). Conversely, systems containing EG as the HBD display lower densities due to its smaller molecular size. Concerning the HBA influence, [Ch]Cl-based DES also provide higher densities than TMAC-based DESs, although the differences depend more on the HBD combination.

The performance of soft-SAFT utilizing the optimized parameters outlined in Table 1 to describe the density of the investigated DESs is also illustrated in Fig. 2. To address the minor discrepancies in mixture density predictions from pure compound parameters, a binary parameter $\eta_{[Ch]Cl\text{-}LA} = 0.93$ was introduced for [Ch]CL:LA (1:2.55) + 10 wt% water and $\eta_{TMAC\text{-}HBD} = 1.023$ for both TMAC-based DESs. Still, this minor correction, with a temperature-independent common coefficient, ensures quantitative agreement across both TMAC-based DESs. In general, the results demonstrate very good agreement between the experimental data and those calculated with soft-SAFT, with an %AAD of 1.12 %, 1.51 %, 2.15 %, 1.16 % and 1.13 % for [Ch]Cl:GL (1:3) + 10 wt% water, TMAC:GL (1:3), [Ch]CL:LA (1:2.55) + 10 wt% water, [Ch]Cl:EG (1:3) and TMAC:EG (1:3), respectively.

Viscosity

Another property of interest for using DESs as solvents in diverse applications is their viscosity, which plays a critical role in fluid dynamics and transfer of mass and heat, affecting their suitability for applications [57–60]. For instance, this property significantly influences the energy required for pumping procedures and the efficiency of gas absorption processes when DESs are utilized as absorbents [61,62]. The viscosity measurements for the TMAC based DESs can be found in Table S4 of the Supporting Information, while in Fig. 3 these results are plotted along with previous [Ch]Cl-based DESs. At standard ambient temperature (298.15 K), noticeable differences in viscosity among DESs were observed. Notably, TMAC:GL (1:3) exhibited the highest viscosity, surpassing 250 mPa·s. This rise in viscosity is attributed to the more elevated number of hydroxyl groups of GL compared to EG, facilitating enhanced hydrogen bonding interactions with TMAC and, consequently, leading to higher viscosity levels.

The experimental data have also been theoretically modeled using the Free-Volume Theory (FVT) coupled with soft-SAFT, applying the spider-web methodology [63] to fit the FVT parameters for the compounds forming the examined DESs using mixture data. The density values required to apply FVT were calculated through the soft-SAFT EoS utilizing the parameters outlined in Table 1. The optimized parameters for DESs forming molecules are included in Table 2.

As can be seen, an excellent agreement between the model and the viscosity data has been found (lines of Fig. 3), with an AAD% of 8.11 %. The major deviations correspond to the lowest temperatures, where the uncertainty of the viscosity measurements is higher. The soft-SAFT plus FVT model offers a poorer performance at low temperature, as seen in previous works [49,64], which can be attributed to the difficulty in capturing the sharp exponential increase in viscosity. However, these deviations only occur at high viscosity values, in a region which is not of interest for practical applications. Otherwise, the description of aqueous DESs is remarkable, reconfirming the high versatility of the approach in achieving a reliable description of this property at different conditions [49].

Table 3
Vapor-liquid equilibria of the selected DESs with HFCs at 300.15 K.

TMAC: GL (1:3)							
R-32		R-125		R-134a		R-143a	
P (MPa)	x_i	P (MPa)	x_i	P (MPa)	x_i	P (MPa)	x_i
0.086	0.006	0.100	0.001	0.064	0.002	0.096	0.002
0.145	0.022	0.193	0.003	0.091	0.004	0.193	0.003
0.222	0.026	0.255	0.004	0.183	0.006	0.284	0.005
0.287	0.043	0.382	0.005	0.274	0.012	0.482	0.007
0.362	0.053	0.481	0.006	0.358	0.016	0.579	0.010
TMAC: EG (1:3)							
R-32		R-125		R-134a		R-143a	
P (MPa)	x_i	P (MPa)	x_i	P (MPa)	x_i	P (MPa)	x_i
0.064	0.016	0.089	0.005	0.069	0.013	0.090	0.005
0.105	0.035	0.168	0.011	0.131	0.027	0.174	0.010
0.147	0.053	0.256	0.016	0.194	0.040	0.258	0.015
0.196	0.071	0.336	0.022	0.261	0.054	0.344	0.019
0.237	0.086			0.271	0.056	0.427	0.026

Solubility of HFCs in [Ch]Cl and TMAC based-DESs

Once the density and viscosity of the investigated DESs has been characterized, their capacity to absorb the most common refrigeration hydrofluorocarbons (in this case, the R-32, R-134a, R-143a, and R-125) is studied. The absorption equilibrium isotherms were measured at 300.15 K under pressures up to 6.5 bar, not to surpass the saturation pressure of R-134a, which stands at 7.0 bar at 300.15 K [65]. The experimental solubility data for the two TMAC-based DESs studied in this work are provided in Table 3, while Fig. 4 represents the equilibrium gas pressure at 300.15 K as a function of the mole fraction of dissolved F-gas (x_{F-gas}) in each DES, including the previous results obtained for [Ch]Cl-based DESs, along with their modelling.

A comprehensive analysis of the results demonstrated a relatively low solubility of HFCs for all DESs investigated here, which can be attributed to the absence of fluorine atoms in their chemical structure. Previous works on the solubility of HFCs in fluorinated ionic liquids [42] and DESs [66] had suggested that the presence of fluorine atoms can enhance the F-gases solubility by forming hydrogen bonds (H-F-H), at the price of a more complex synthesis and higher environmental impact. However, this high degree of absorption comes at a cost of a nearly null capacity to selectively separate these HFCs.

In the DESs under investigation in this work, it appears that the primary influence lies on a weak physical absorption dominated by

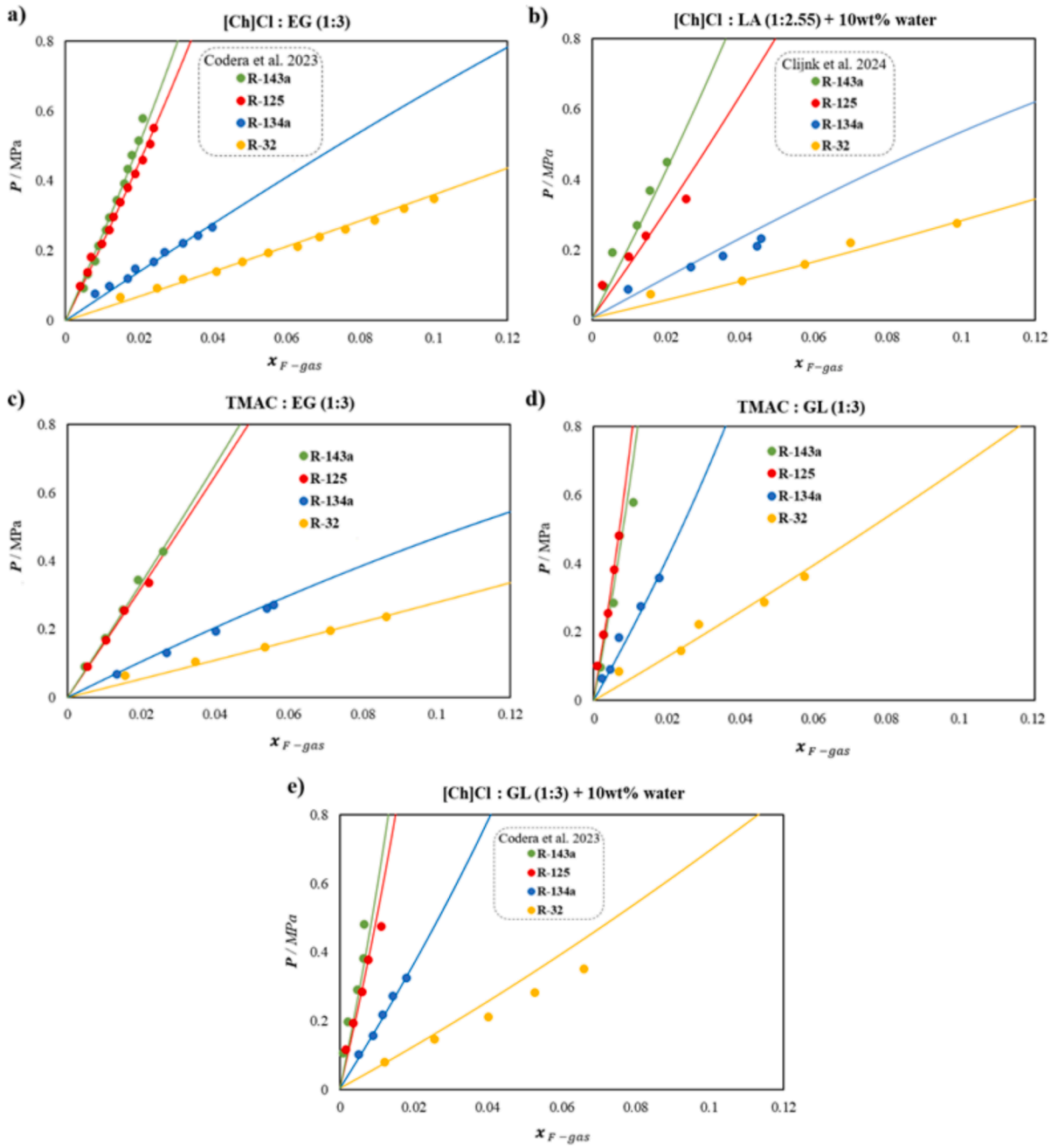

Fig. 4. Vapor-liquid equilibria for the DESs with HFCs at 300.15 K. Symbols correspond to experimental results of this work and literature data [44,45], while the lines are soft-SAFT calculations.

entropic effects, where the volume of the F-gas molecules plays a key role. Indeed, R-32, the smallest HFC among those studied, being the only single-carbon compound (with two fluorine atoms), exhibits the highest solubility. Concerning the two-carbon refrigerants, it may be noted that the amount of fluorine atoms in HFCs do not consistently correlate with enhanced solubility. For instance, while R-134a, containing four fluorine atoms, ranks as the second compound with the highest solubility, R-125 (with five fluorine atoms) and R-143a (with three fluorine atoms) exhibit similar and lower solubility levels compared to other F-gases. In this case, two different effects play a role. On one hand, R-125 has a low solubility due to the presence of five fluorine atoms, forming a relatively stable structure of a certain size and leaving low allocation for strong interactions with the DESs. Conversely, the asymmetric R-143a, with three fluorine atoms at the same molecule end, exhibits a high dipole moment [67], but lacks the previously mentioned H-F-H structure, resulting in a lower solubility. In any case, this variation in solubility among these HFCs represents an advantage for their separation. Specifically, it suggests that R-125 and R-143a could potentially be readily separated from mixtures of HFCs containing R-134a and R-32.

Although the qualitative outcomes among all DESs are somewhat similar, it is notable that TMAC:EG (1:3) exhibits a slightly higher absorption capacity, closely followed by [Ch]CL:LA (1:2.55) + 10 wt% water, and then by [Ch]Cl:EG (1:3), [Ch]Cl:GL (1:3) + 10 wt% water, and finally TMAC:GL (1:3). The latter seems to be clearly affected by its higher viscosity, possibly affecting mass transfer. In any case, no substantial differences are appreciated among all DESs, suggesting that the influence of the DESs structure on the solubilities of the F-gases appears to be modest. However, it is important to remember that the choice of the best solvent will be determined by its selectivity and not by its absorption capacity.

Table 4
Soft-saft energy binary interaction parameter (ξ_{ij}) adjusted.

Compound *i*	Compound *j*	ξ_{ij}
[Ch]Cl	R-143a	1.1374
[Ch]Cl	R-125	1.2103
[Ch]Cl	R-134a	1.1450
[Ch]Cl	R-32	1.2998
TMAC	R-143a	1.0477
TMAC	R-125	1.1278
TMAC	R-134a	1.0577
TMAC	R-32	1.3000
EG	HFCs	1.1008
LA	HFCs	1.2338
GL	HFCs	1.0532
[Ch]Cl	Water	1.0450*
R-134a	Water	0.8500
R-143a	Water	0.8500
R-32	Water	0.8500

*Reference:[49].

The thermodynamic model, as shown in Fig. 4, provides good agreement with the experimental data. The molecular parameters provided in Table 1 are used here to deal with multicomponent calculations, where each combination between DES and HFC is treated as a ternary mixture, except for the corresponding HFC with the DES [Ch]Cl:LA (1:2.55) + 10 wt% water and [Ch]Cl:GL (1:3) + 10 wt% water, which are treated as quaternary systems. Subsequently, the model must account for all possible interactions among the three or four compounds involved. On one side, cross-association interactions between sites are explicitly considered, with only positive–negative interactions being allowed. On the other side, given the very different structure of the molecules involved, it is necessary to apply a correction in the crossed dispersive energy by means of the binary parameter, ξ_{ij} (see Eq. S7 in Section S2 of Supporting Information). No further size corrections are necessary for the Berthelot combining rule with $\eta = 1$ for all binary combinations, with the exception of the TMAC:HBDs and [Ch]Cl:LA DESs (as explained in previous Section), having a constant value of η = 1.023 for TMAC and $\eta = 0.930$ for [Ch]Cl, respectively. A summary of the necessary ξ_{ij} values to quantitatively describe the HFCs solubility in DESs is provided in Table 4.

Some remarkable trends emerge from analyzing the values of these parameters and their relevance to the interactions within the mixture. Notably, most cases exhibit an energy binary parameter ξ_{ij} greater than one, specifically in adjusting the interactions involving the DESs forming molecules and the HFCs. These results suggest that the classical Lorentz-Berthelot combining rules underestimate the solubility of the HFCs in the DESs, indicating potential missing interactions within the model for the investigated mixtures. Interestingly, a consistent ξ_{ij} value is observed across interactions between each HBD and the four HFCs, suggesting that the parameter can be transferred among HFCs if no experimental data are available. For the case of the quaternary mixtures containing water, one parameter between [Ch]Cl and water was transferred from previous work (ξ_{ij} = 1.0450) [49]. In contrast, the parameter for interactions between R-134a, R-143a or R-32 with water was optimized here and fixed at ξ_{ij} = 0.8500. Overall, the soft-SAFT calculations effectively describe the solubility of each HFC in the examined DESs, showing good agreement with experimental data as depicted by the lines in Fig. 4 (individual deviation values are available in Table S5 of the Supporting Information).

Enthalpy and entropy of dissolution

The absorption of HFCs into the DESs does involve examining additional thermodynamic metrics, apart from solubility, such as the absorption enthalpy and entropy. These metrics provide insights into the strength of the interactions and the degree of order when a gas is dissolved into the solvent, respectively [68]. Their values under different constant compositions can be determined utilizing data derived from the soft-SAFT EoS, according to the following equations:

$$\Delta H_{dis} = -RT^2\left(\frac{d\ln P_i}{dT}\right)_{x_i} \quad (1)$$

$$\Delta S_{dis} = -RT\left(\frac{d\ln P_i}{dT}\right)_{x_i} \quad (2)$$

where ΔH_{dis} is the molar enthalpy of absorption; ΔS_{dis} is the molar entropy of absorption; R is the universal gas constant (8.3145 J.mol^{-1}.K^{-1}); P_i is the partial pressure of the dissolved gas i; T is overall system temperature and x_i is the mole fraction of the dissolved gas i in the DESs, which is fixed at 0.0001 (a very low gas concentration). The results for each HFC within the respective DESs are provided in Table 5.

As can be seen in Table 5, R-32 exhibits the highest negative values of ΔH_{dis} among the HFCs, which implies that all investigated DESs have a higher affinity for R-32 than for the other HFCs studied. Regarding the results of ΔS_{dis}, negative values are found in all cases, stemming from the gas's condensation. The decrease in entropy caused by this phase transition is not compensated by the entropy generated from the disruption of the HFCs into the organized structure of the DESs.

Selectivity and absorption calculations

The ability of an absorbent to selectively capture a specific F-gas from a blend is crucial for tailoring gas recycling and separation processes. Thus, the ideal selectivity of each HFC within the respective DESs is used to pre-screen their efficiency in separating binary HFCs mixtures. The ideal selectivity at infinite dilution, denoted as α, relates the amount of the HFC dissolved in the DES at an isotherm set and is expressed as the ratio of Henry's law constants between the two pure HFCs [69]. Following this, the soft-SAFT EoS is employed to predict pressure data as solubility approaches zero for each isotherm and compound. These predictions enable the computation of the ideal selectivity for two specific refrigerants i and j in terms of Henry's law constants, as follows:

$$\alpha_{i/j}{}^{T} = \frac{k^{j}_{\mathrm{H,\,eff}}{}^{T}}{k^{i}_{\mathrm{H,eff}}{}^{T}} = \frac{\lim_{x_j\to 0}\left(\frac{P}{x_j}\right)^{T}}{\lim_{x_i\to 0}\left(\frac{P}{x_i}\right)^{T}} \quad (3)$$

where $k^{i}_{H,eff}$ signifies effective Henry's law constant [70] for gas i at temperature T, while x_i denotes the mole fraction of compound i in the liquid. Lastly, $\alpha_{i/j}$ represents the ideal selectivity at infinite dilution of

Table 5
Calculated enthalpy and entropy of dissolution for HFCs in DESs at 300.15 K and x_i = 0.0001.

DES	ΔH_{dis}/kJ.mol^{-1}				ΔS_{dis}/J.K^{-1}.mol^{-1}			
	R- 143a	R-125	R-134a	R-32	R- 143a	R-125	R-134a	R-32
TMAC:GL (1:3)	−8.00	−7.55	−11.35	−14.15	−25.36	−23.92	−35.96	−44.84
[Ch] Cl:GL (1:3) + 10 wt% H_2O	−30.00	−30.58	−34.90	−37.05	−95.06	−96.89	−110.6	−117.4
[Ch] Cl:EG (1:3)	−11.28	−11.60	−17.28	−21.51	−35.74	−36.74	−54.76	−68.16
[Ch] Cl:LA(1:2.55) + 10 wt% H_2O	−35.35	−35.97	−37.37	−37.85	−111.9	−113.9	−118.4	−119.9
TMAC:EG (1:3)	−11.06	−11.17	−17.13	−21.60	−35.05	−35.38	−54.26	−68.44

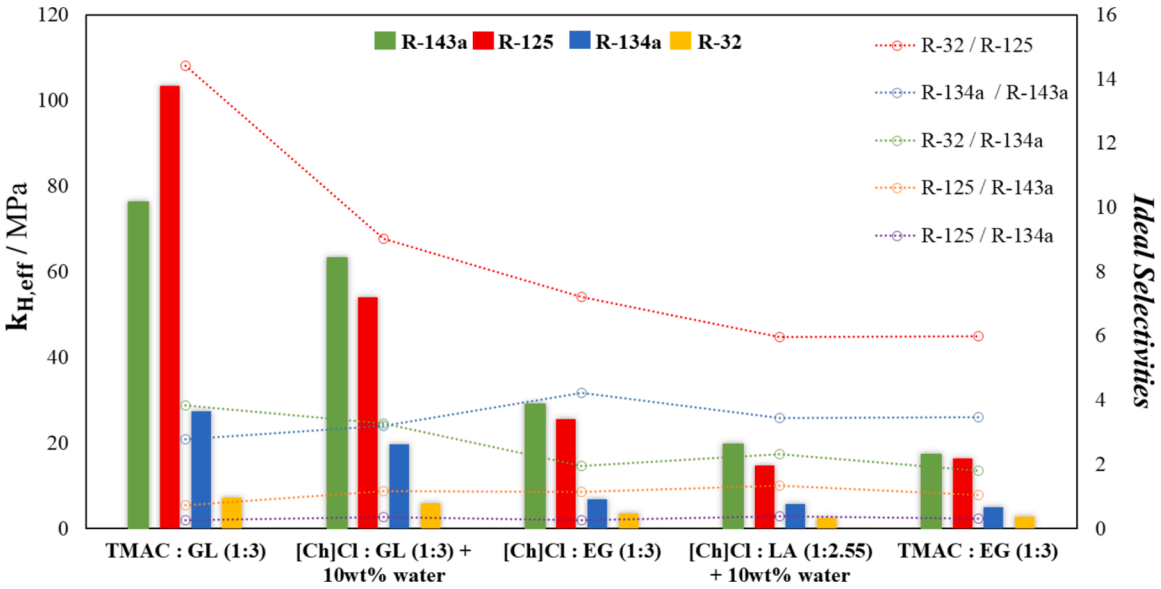

Fig. 5. Calculated effective Henry's constants ($k_{H,eff}$) for HFCs (bars graph, left axis) and ideal selectivity ($\alpha_{i/j}$, symbols and lines, right axis) in TMAC:GL (1:3), [Ch]Cl:GL (1:3) + 10 wt% water, [Ch]Cl:EG (1:3), [Ch]CL:LA (1:2.55) + 10 wt% water and TMAC:EG (1:3) at 300.15 K.

the compound *j* with respect to the compound *i*. The ideal selectivity obtained for a temperature of 300.15 K is plotted in Fig. 5, where the effective Henry's law constants are visually illustrated in the same figure and listed in Table S6 of Supporting Information.

The values of effective Henry's constants are directly linked to the results observed for the solubility measurements. TMAC:EG (1:3) shows the lowest $k_{H,eff}$, indicating the highest absorption capacity, followed by [Ch]CL:LA (1:2.55) + 10 wt% water, [Ch]Cl:EG (1:3), [Ch]Cl:GL (1:3) + 10 wt% water, and finally TMAC:GL (1:3), which exhibits the highest $k_{H,eff}$ for all HFCs. Additionally, it is evident that, for all DESs, R-32 has the lowest $k_{H,eff}$, followed by R-134a, while higher $k_{H,eff}$ values are consistently observed for R-125 and R-143a across all DESs [43].

Concerning the ideal selectivity, Fig. 5 also illustrates the selectivity for the binary mixtures R-32/R-125, R-134a/R-143a, R-32/R-134a, R-125/R-143a and R-125/R-134a at 300.15 K. Despite lower absorption capacities compared to fluorinated DESs [43,66], the DESs investigated in this study exhibit commendable selectivities for certain HFCs mixtures. The highest values (ranging between 5.98 and 14.4) are obtained for the R-32/R-125 mixtures with the studied DESs, with TMAC:GL (1:3) having the best selectivity, indicating its preference for R-32 in this system. For the R-134a/R-143a mixture, the selectivity ranges between 2.78 and 3.46, with [Ch]Cl:EG (1:3) yielding the highest value. Unfortunately, none of the DESs considered in this work seems appropriate to separate R-125 from R-143a, as it was previously inferred from the solubility figures.

The ideal selectivity calculated from effective Henry's coefficients is an approximation based on the infinite dilution behavior of pure compounds (i.e., HFCs in this study), which does not consider the competition between the gases and is solely used to provide a first qualitative approximation on the separation capacity for each DESs. Based on this preliminary information, a more accurate assessment of the gas separation efficiency needs to be performed by studying the competitive selectivity to recover the compounds from multicomponent commercial refrigeration blends, including R410A (with 70.583 mol% R-32 and 29.417 mol% R-125), R407F (with 48.299 mol% R-32, 20.129 mol% R-125, and 31.572 mol% R-134a), and R404A (with 35.782 mol% R-125, 60.392 mol% R-143a, and 3.826 mol% R-134a).

In this case, the values of competitive selectivities ($S_{i/j}$) calculated for these gas mixtures are obtained throughout Eq. (4).

$$S_{i/j} = \frac{y_j/x_j}{y_i/x_i} \tag{4}$$

where *x* is the mole fraction of each component in the liquid phase, and *y* is the mole fraction of each component in the gas phase. However, the

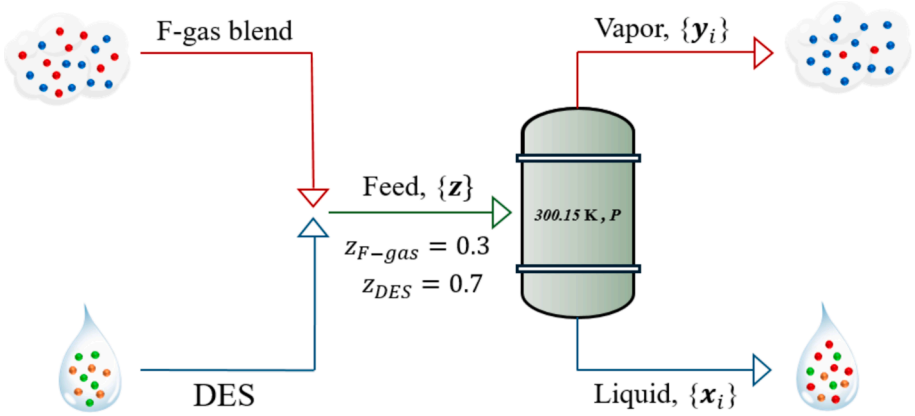

Fig. 6. Illustration of liquid–vapor flash calculations via soft-SAFT EoS depicting the separation performance of commercial refrigerant blends at 300.15 K and various pressures (1, 5, and 10 bar).

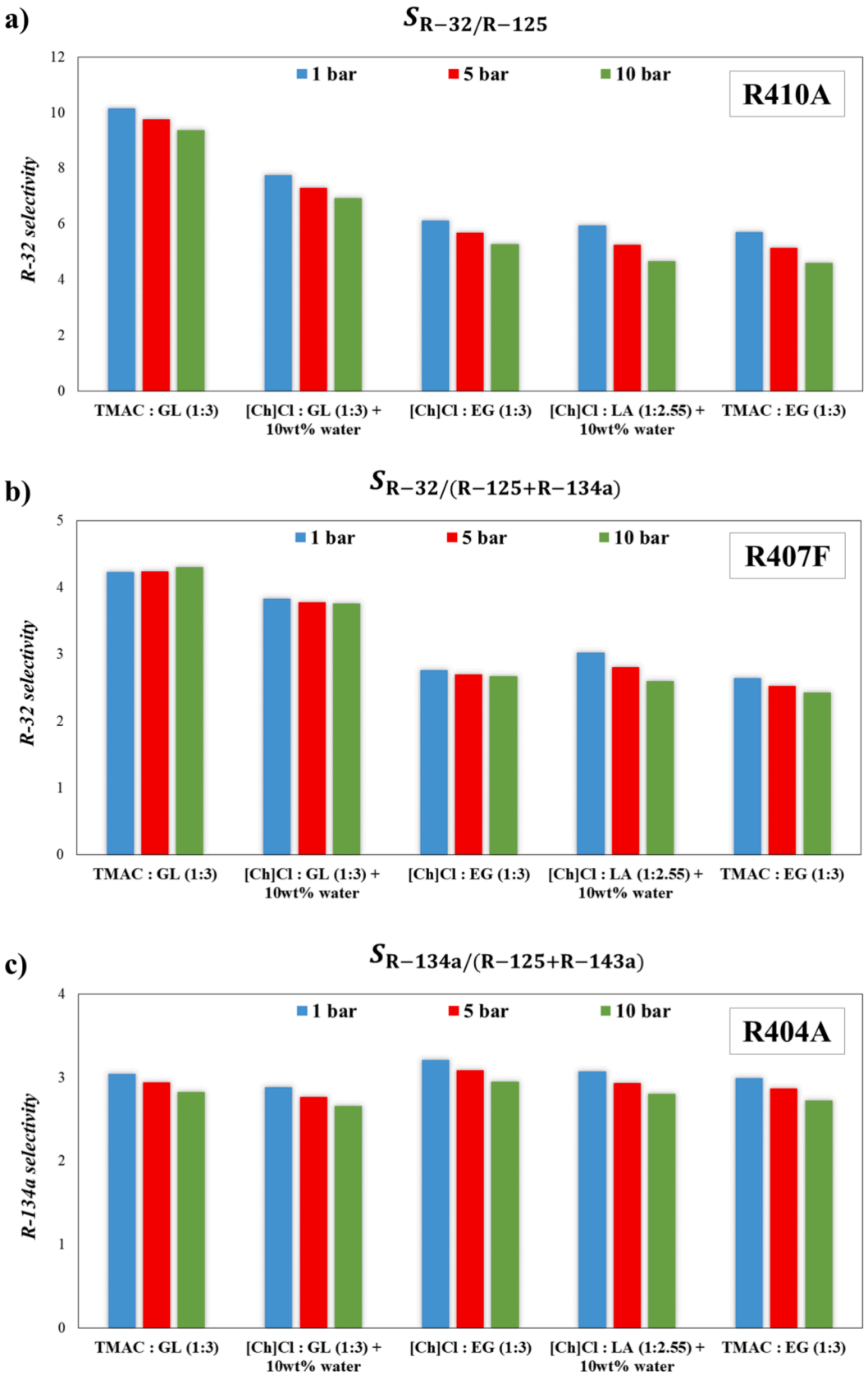

Fig. 7. Competitive selectivity of refrigerant blends in DESs at 300.15 K and different pressures, for a mixture with a global composition of $z_{DES} = 0.7$ and $z_{F-gas\ blend} = 0.3$ modeled using soft-SAFT EoS for **a)** R-32 recovery from R410A blend, **b)** R-32 recovery from R407F blend and **c)** R-134a recovery from R404A blend.

intrinsic nature of Eq. (4) is originally thought for a binary comparison and needs to be adapted for ternary gas mixtures (R407F and R404A). In that case, we have opted to define the selectivity of one gas over the other two by considering the non-desired gases as a single entity "GAS_m", where the x_{GAS_m} is the sum of their liquid mole fractions, and y_{GAS_m} represents the sum of their vapor mole fractions. For instance, in a mixture comprising three gases (GAS_1, GAS_2, and GAS_3), the equation to determine the selectivity (S) of GAS_1 over the other two gases would be as follows:

$$x_{GASm} = x_{GAS_2} + x_{GAS_3} \tag{5}$$

$$y_{GASm} = y_{GAS_2} + y_{GAS_3} \tag{6}$$

$$S_{GAS_1/GAS_m} = \frac{y_{GASm}/x_{GAS_m}}{y_{GAS_1}/x_{GAS_1}} \tag{7}$$

The equilibrium compositions in Eqs. (4) and (7) are obtained from liquid-vapor flash calculations using soft-SAFT EoS, which are computed by an iterative process that involves solving a flash model into the Rachford-Rice equation [71]. This calculation considers an initial global composition with a DES mole fraction of 0.7 ($z_{DES} = 0.7$) and 0.3 for the corresponding HFCs blend ($z_{F-gas} = 0.3$), the latter with the commercial proportions previously stated, at the desired operating pressure and 300.15 K, as illustrated in Fig. 6.

The separation performance of R-32 and R-134a from three commercial refrigerant blends at 300.15 K and the investigated − pressures is shown in Fig. 7. Additionally, the selectivity between the other two gases for the ternary HFCs blends R407F and R404A are illustrated in Figs. S2 and S3 in the Supporting Information.

An analysis of Fig. 7 reveals that a high separation efficiency can be achieved to separate R410A compounds, with TMAC:GL (1:3) demonstrating the best performance, as seen in Fig. 7a. Moreover. Fig. 7b demonstrates the competitive selectivity for separating R-32 from the R407F blend (i.e. so when adding R-134a, forming a ternary system). Finally, no significant differences are appreciated when extracting R-134a from R404A blend (in the presence of R-125 and R-143a), with a slightly better performance of [Ch]Cl:EG (1:3) and [Ch]CL:LA (1:2.55) + 10 wt% water over the rest (see Fig. 7c).

In general terms, the predicted competitive selectivity aligns with the ideal selectivity at infinite dilution from Fig. 5, particularly at low pressure, where ideal conditions apply. However, on the one hand, while lower pressures enhance separation performance, this comes at the cost of a reduced sorption capacity, as can be seen in Fig. 4, and consequently a lower recovery. On the other hand, high-pressure conditions do not seem to be attractive, as they lead to decreased separation performance for specific DESs. Therefore, according to this analysis, operating under moderate pressure conditions is advisable for an efficient separation of HFCs. Another crucial factor for the effective application of DESs is their thermal stability, particularly when high temperature desorption processes are applied. It is important to consider that DESs may experience thermal decomposition and volatilization at high temperatures or vacuum pressures [72,73]. DESs are generally regarded as low-volatility solvents; however, they may still volatilize under ambient temperature and pressure conditions, potentially impacting their long-term performance [74]. HBDs play a crucial role in the thermal stability of DESs, as they tend to decompose or volatilize first due to their relatively lower thermal stability or boiling point compared to the HBA. Although the thermal stability of the DESs studied here has not been directly assessed, we can infer that, ideally, the stability of [Ch]Cl-based DESs will decrease in the order GL > EG > LA, based on the boiling points of these HBDs [72]. A similar analysis can be applied to TMAC-based DESs. However, this conclusion should be experimentally confirmed, as the HBA:HBD ratio also affects molecular interactions and overall thermal stability. Thus, for an industrial application of these DESs, a balanced approach that considers both moderate pressure and thermal stability is vital for optimizing the separation of HFCs.

These findings offer a valuable insight into the thermodynamic behavior in mixtures comprised of HFCs and type III DESs. However, the development and implementation of an efficient separation process for the recovery of F-gases should include additional considerations, such as recycling stability, economic evaluation and life cycle analysis [75]. Although such studies lie out of the scope of this work, the obtained results offer a consistent thermodynamic model, which can be utilized in the design and evaluation of new processes.

Conclusions

In this study, the solubility of four common F-gases, particularly HFCs, (R-125, R-134a, R-32, and R143a) was investigated using three DESs based on [Ch]-Cl, employing ethylene glycol, glycerol, and lactic acid as HBDs, and two DESs based on TMAC utilizing ethylene glycol and glycerol as HBDs, at 300.15 K and low pressure. A comprehensive thermodynamic characterization of the HFCs absorption capability within these DESs was performed using the soft-SAFT EoS. Generally, the solubility trend across the DESs was observed as R-32 > R-134a > R-125 ≈ R-143a. Among the DESs studied, TMAC:EG (1:3) showed a higher affinity for the studied HFCs, presenting a slightly higher absorption capacity. Despite a relatively low absorption, the DESs investigated exhibited promising selectivity for separating HFCs mixtures, particularly those containing R-32, thereby suggesting potential applications in separating commercial blends like R410A and R407F. The detailed thermodynamic modeling further supports the applicability of the soft-SAFT equation in accurately describing these systems, facilitating the prediction of various crucial properties for process design and scale-up, including density and viscosity of pure DESs, enthalpy and entropy of dissolution, effective Henry's constants, as well as ideal and competitive selectivity. In particular, the selectivity analysis allows the identification of the more suitable candidates among the studied DES for recovering R-32, R-134a, and R-125 from commercial HFCs blends, including R410A, R407F, and R404A. These findings offer valuable insights for developing and implementing efficient separation processes for HFCs, contributing to sustainability efforts in refrigeration.

CRediT authorship contribution statement

L.V.T.D. Alencar: Writing – original draft, Investigation, Data curation. **B. González-Barramuño:** Software, Methodology, Investigation. **S.B. Rodriguez-Reartes:** Writing – review & editing, Supervision. **H. Quinteros-Lama:** Writing – review & editing, Methodology. **J.M. Garrido:** Validation, Supervision. **V. Codera:** Validation, Data curation. **J.O. Pou:** Validation, Data curation. **F.W. Tavares:** Writing – review & editing, Funding acquisition. **R. Gonzalez-Olmos:** Writing – review & editing, Resources, Methodology. **F. Llovell:** Writing – review & editing, Supervision, Project administration, Funding acquisition.

Declaration of competing interest

The authors declare that they have no known competing financial interests or personal relationships that could have appeared to influence the work reported in this paper.

Acknowledgments

The authors would like to thank the master student Daniel Clijnk for his support in the lab. The authors also thank Dr. Angel Gutiérrez Ortega from the company GRIT, Gases, Research, Innovation & Technology S.L. U. for his help with the materials supply. This research is supported by projects STOP-F-Gas (PID2019-108014RB-C21) and NEW-F-TECH (TED2021-130959B-I00) funded by the Spanish Ministry of Science and Innovation MCIN/AEI/10.13039/501100011033/ and the European Union NextGenerationEU/PRTR, as well as by project CIRCFGAS (2023-URL-Proj-053) funded by Department of Research and

Universities of Generalitat de Catalunya and Universitat Ramon Llull. Additional funding by the European Union, Next Generation EU, within the framework of the Recovery, Transformation, and Resilience Plan "Investigo Program" for the hiring of young job seekers for the development and execution of research and innovation functions, tasks, and initiatives, is appreciated. H. Quinteros-Lama and J. M Garrido acknowledge further funding by FONDECYT, Chile (Project 1230236 and 1240765). L.V.T.D. Alencar thanks CAPES (Coordination for the Improvement of Higher Education Personnel) for financial support. S.B. Rodriguez-Reartes acknowledges the financial support of the "María Zambrano" grant awarded by Universitat Rovira i Virgili for the requalification of the Spanish university system for 2021-2023. Finally, recognition from AGAUR as Consolidated Research Groups for GESPA (2021 SGR 00321) and AGACAPE (SGR 2021-00738) are gratefully appreciated.

Appendix A. Supplementary data

Supplementary data to this article can be found online at https://doi.org/10.1016/j.jiec.2024.12.005.

References

[1] L. Hoesung, IPCC, 2023: Climate Change 2023: Synthesis Report. Contribution of Working Groups I, II and III to the Sixth Assessment Report of the Intergovernmental Panel on Climate Change, Journal, IPCC, Geneva, Switzerland, pp. 35-115. doi: 10.59327/IPCC/AR6-9789291691647.
[2] NOAA Global Monitoring Laboratory, The NOAA Annual Grenhouse Gas Index (AGGI), Mar. 05, 2024 [Online]. Available:https://gml.noaa.gov/aggi/aggi.html.
[3] EPA: United States Environmental Protection Agency, Inventory of U.S. greenhouse gas emissions and sinks: 1990-2018, 2020.
[4] M.J. Molina, F.S. Rowland, Stratospheric sink for chlorofluoromethanes: chlorine atom-catalysed destruction of ozone, Nature 249 (1974) 810–812, https://doi.org/10.1038/249810a0.
[5] IPCC, Climate Change 2022: Mitigation of Climate Change, Journal, 2024.
[6] European Parliament and Council, Amendment to the Montreal protocol on substances that deplete the ozone layer, 2016.
[7] G.J.M. Velders, J.S. Daniel, S.A. Montzka, I. Vimont, M. Rigby, P.B. Krummel, J. Muhle, S. O'Doherty, R.G. Prinn, R.F. Weiss, D. Young, Projections of hydrofluorocarbon (HFC) emissions and the resulting global warming based on recent trends in observed abundances and current policies, Atmos. Chem. Phys. 22 (2022) 6087–6101, https://doi.org/10.5194/acp-22-6087-2022.
[8] B.K. Sovacool, S. Griffiths, J. Kim, M. Bazilian, Climate change and industrial F-gases: A critical and systematic review of developments, sociotechnical systems and policy options for reducing synthetic greenhouse gas emissions, Renew. Sustain. Energy Rev. 141 (2021) 110759, https://doi.org/10.1016/j.rser.2021.110759.
[9] European Commission Climate Action, Fluorinated Greenhouse Gases (2019).
[10] D.J. Sheldon, M.R. Crimmin, Repurposing of F-gases: challenges and opportunities in fluorine chemistry, Chem. Soc. Rev. 51 (2022) 4977–4995, https://doi.org/10.1039/D1CS01072G.
[11] P.J. Castro, J.M.M. Aráujo, G. Martinho, A.B. Pereiro, Waste Management Strategies to Mitigate the Effects of Fluorinated Greenhouse Gases on Climate Change, Appl. Sci. 11 (2021) 4367, https://doi.org/10.3390/app11104367.
[12] G. Morrison, M.O. McLinden, Azeotropy in refrigerant mixtures: Azéotropie dans les mélanges de frigorigènes, Int. J. Refrig 16 (1993) 129–138, https://doi.org/10.1016/0140-7007(93)90069-K.
[13] D. Han, K.H. Row, Recent Applications of Ionic Liquids in Separation Technology, Molecules 15 (2010) 2405–2426, https://doi.org/10.3390/molecules15042405.
[14] S. Asensio-Delgado, F. Pardo, G. Zarca, A. Urtiaga, Absorption separation of fluorinated refrigerant gases with ionic liquids: Equilibrium, mass transport, and process design, Sep. Purif. Technol. 276 (2021) 119363, https://doi.org/10.1016/j.seppur.2021.119363.
[15] Z. Lei, C. Dai, J. Zhu, B. Chen, Extractive distillation with ionic liquids: A review, AIChE J 60 (2014) 3312–3329, https://doi.org/10.1002/aic.14537.
[16] L.F. Vega, O. Vilaseca, F. Llovell, J.S. Andreu, Modeling ionic liquids and the solubility of gases in them: Recent advances and perspectives, Fluid Phase Equilib. 294 (2010) 15–30, https://doi.org/10.1016/j.fluid.2010.02.006.
[17] E.L. Smith, A.P. Abbott, K.S. Ryder, Deep Eutectic Solvents (DESs) and Their Applications, Chem. Rev. 114 (2014) 11060–11082, https://doi.org/10.1021/cr300162p.
[18] A. Prabhune, R. Dey, Green and sustainable solvents of the future: Deep eutectic solvents, J. Mol. Liq. 379 (2023) 121676, https://doi.org/10.1016/j.molliq.2023.121676.
[19] T. Lemaoui, A. Boublia, A.S. Darwish, M. Alam, S. Park, B.-H. Jeon, F. Banat, Y. Benguerba, I.M. AlNashef, Predicting the Surface Tension of Deep Eutectic Solvents Using Artificial Neural Networks, ACS Omega 7 (2022) 32194–32207, https://doi.org/10.1021/acsomega.2c03458.
[20] L.V.T.D. Alencar, S.B. Rodríguez-Reartes, F.W. Tavares, F. Llovell, Assessing Viscosity in Sustainable Deep Eutectic Solvents and Cosolvent Mixtures: An Artificial Neural Network-Based Molecular Approach, ACS Sustain. Chem. Eng. (2024), https://doi.org/10.1021/acssuschemeng.3c07219.
[21] A. Boublia, T. Lemaoui, F. Abu Hatab, A.S. Darwish, F. Banat, Y. Benguerba, I. M. AlNashef, Molecular-based artificial neural network for predicting the electrical conductivity of deep eutectic solvents, J. Mol. Liq. (2022) 120225, https://doi.org/10.1016/j.molliq.2022.120225.
[22] D. Shi, F. Zhou, W. Mu, C. Ling, T. Mu, G. Yu, R. Li, Deep insights into the viscosity of deep eutectic solvents by an XGBoost-based model plus SHapley Additive exPlanation, PCCP 24 (2022) 26029–26036, https://doi.org/10.1039/D2CP03423A.
[23] F. Zhou, D. Shi, W. Mu, S. Wang, Z. Wang, C. Wei, R. Li, T. Mu, Machine learning models accelerate deep eutectic solvent discovery for the recycling of lithium-ion battery cathodes, Green Chem. 26 (2024) 7857–7868, https://doi.org/10.1039/D4GC01418A.
[24] H.S. Salehi, R. Hens, O.A. Moultos, T.J.H. Vlugt, Computation of gas solubilities in choline chloride urea and choline chloride ethylene glycol deep eutectic solvents using Monte Carlo simulations, J. Mol. Liq. 316 (2020) 113729, https://doi.org/10.1016/j.molliq.2020.113729.
[25] D.V. Wagle, L. Adhikari, G.A. Baker, Computational perspectives on structure, dynamics, gas sorption, and bio-interactions in deep eutectic solvents, Fluid Phase Equilib. 448 (2017) 50–58, https://doi.org/10.1016/j.fluid.2017.04.018.
[26] G. Li, C. Gui, C. Dai, G. Yu, Z. Lei, Molecular Insights into SO2 Absorption by [EMIM][Cl]-Based Deep Eutectic Solvents, ACS Sustain. Chem. Eng. 9 (2021) 13831–13841, https://doi.org/10.1021/acssuschemeng.1c04639.
[27] R. Abedin, S. Heidarian, J.C. Flake, F.R. Hung, Computational Evaluation of Mixtures of Hydrofluorocarbons and Deep Eutectic Solvents for Absorption Refrigeration Systems, Langmuir 33 (2017) 11611–11625, https://doi.org/10.1021/acs.langmuir.7b02003.
[28] P. Khan, M. Yasin, H. AlMohamadi, X. Zhang, A. Laeeq Khan, R. Nawaz, M. Amjad Gilani, Exploring the potential of hydrophobic deep eutectic solvents for bioethanol separation using DFT and COSMO-RS model, J. Mol. Liq. (2024) 123665, https://doi.org/10.1016/j.molliq.2023.123665.
[29] R. Ullah, M. Atilhan, B. Anaya, M. Khraisheh, G. García, A. ElKhattat, M. Tariq, S. Aparicio, A detailed study of cholinium chloride and levulinic acid deep eutectic solvent system for CO2 capture via experimental and molecular simulation approaches, PCCP 17 (2015) 20941–20960, https://doi.org/10.1039/C5CP03364K.
[30] W.G. Chapman, K.E. Gubbins, G. Jackson, M. Radosz, New reference equation of state for associating liquids, Ind. Eng. Chem. Res. 29 (1990) 1709–1721, https://doi.org/10.1021/ie00104a021.
[31] S.H. Huang, M. Radosz, Equation of state for small, large, polydisperse, and associating molecules, Ind. Eng. Chem. Res. 29 (1990) 2284–2294, https://doi.org/10.1021/ie00107a014.
[32] I. Polishuk, A. Chiko, E. Cea-Klapp, J.M. Garrido, Implementation of CP-PC-SAFT and CS-SAFT-VR-Mie for Predicting the Thermodynamic Properties of C1–C3 Halocarbon Systems. II. Inter-Relation between Solubilities in Ionic Liquids, Their Pressure, Volume, and Temperature, and Critical Constants, Ind. Eng. Chem. Res. 60 (2021) 13084–13093, https://doi.org/10.1021/acs.iecr.1c02720.
[33] A. Galindo, A. Gil-Villegas, P.J. Whitehead, G. Jackson, A.N. Burgess, Prediction of Phase Equilibria for Refrigerant Mixtures of Difluoromethane (HFC-32), 1,1,1,2-Tetrafluoroethane (HFC-134a), and Pentafluoroethane (HFC-125a) Using SAFT-VR, J. Phys. Chem. B 102 (1998) 7632–7639, https://doi.org/10.1021/jp9809437.
[34] M. Lampe, M. Stavrou, J. Schilling, E. Sauer, J. Gross, A. Bardow, Computer-aided molecular design in the continuous-molecular targeting framework using group-contribution PC-SAFT, Comput. Chem. Eng. 81 (2015) 278–287, https://doi.org/10.1016/j.compchemeng.2015.04.008.
[35] O. Vilaseca, F. Llovell, J. Yustos, R.M. Marcos, L.F. Vega, Phase equilibria, surface tensions and heat capacities of hydrofluorocarbons and their mixtures including the critical region, J. Supercrit. Fluids 55 (2010) 755–768, https://doi.org/10.1016/j.supflu.2010.10.015.
[36] C. Avendaño, T. Lafitte, C.S. Adjiman, A. Galindo, E.A. Müller, G. Jackson, SAFT-γ Force Field for the Simulation of Molecular Fluids: 2, Coarse-Grained Models of Greenhouse Gases, Refrigerants, and Long Alkanes, the Journal of Physical Chemistry B 117 (2013) 2717–2733, https://doi.org/10.1021/jp306442b.
[37] C.G. Albà, L.F. Vega, F. Llovell, A consistent thermodynamic molecular model of n-hydrofluoroolefins and blends for refrigeration applications, Int. J. Refrig 113 (2020) 145–155, https://doi.org/10.1016/j.ijrefrig.2020.01.008.
[38] F.J. Blas, L.F. Vega, Thermodynamic behaviour of homonuclear and heteronuclear Lennard-Jones chains with association sites from simulation and theory, Mol. Phys. 92 (1997) 135–150, https://doi.org/10.1080/00268979709482082.
[39] C.G. Albà, I.I.I. Alkhatib, F. Llovell, L.F. Vega, Assessment of Low Global Warming Potential Refrigerants for Drop-In Replacement by Connecting their Molecular Features to Their Performance, ACS Sustain. Chem. Eng. 9 (2021) 17034–17048, https://doi.org/10.1021/acssuschemeng.1c05985.
[40] I.I.I. Alkhatib, C.G. Albà, A.S. Darwish, F. Llovell, L.F. Vega, Searching for Sustainable Refrigerants by Bridging Molecular Modeling with Machine Learning, Ind. Eng. Chem. Res. 61 (2022) 7414–7429, https://doi.org/10.1021/acs.iecr.2c00719.
[41] C.G. Albà, I.I.I. Alkhatib, F. Llovell, L.F. Vega, Hunting sustainable refrigerants fulfilling technical, environmental, safety and economic requirements, Renew. Sustain. Energy Rev. 188 (2023) 113806, https://doi.org/10.1016/j.rser.2023.113806.
[42] D. Jovell, S.B. Gómez, M.E. Zakrzewska, A.V.M. Nunes, J.M.M. Araújo, A. B. Pereiro, F. Llovell, Insight on the Solubility of R134a in Fluorinated Ionic Liquids

and Deep Eutectic Solvents, J. Chem. Eng. Data 65 (2020) 4956–4969, https://doi.org/10.1021/acs.jced.0c00588.
[43] M.G. Demirbek, S.B. Rodriguez Reartes, F. Llovell, Thermodynamic Analysis of the Absorption of Common Refrigerants in Fluorinated Deep Eutectic Solvents, Fluid Phase Equilib. (2024) 114077, https://doi.org/10.1016/j.fluid.2024.114077.
[44] V. Codera, D. Clijnk, J.O. Pou, J. Fernandez-Garcia, F. Llovell, R. Gonzalez-Olmos, Process design for the recovery of waste refrigerants using deep eutectic solvents, J. Environ. Chem. Eng. 11 (2023) 110255, https://doi.org/10.1016/j.jece.2023.110255.
[45] V.C.D. Clijnk, J.O. Pou, J. Fernandez-Garcia, R. Gonzalez-Olmos, Enhancing Circular Economy of Waste Refrigerants Management using Deep Eutectic Solvents, Sustain. Mater. Technol. 41 (2024), https://doi.org/10.1016/j.susmat.2024.e01062.
[46] X. Li, K.H. Row, Development of deep eutectic solvents applied in extraction and separation, J. Sep. Sci. 39 (2016) 3505–3520, https://doi.org/10.1002/jssc.201600633.
[47] H. Moradi, N. Farzi, Experimental and computational assessment of the physicochemical properties of choline chloride/ ethylene glycol deep eutectic solvent in 1:2 and 1:3 mole fractions and 298.15–398.15 K, J. Mol. Liq. (2021) 116669, https://doi.org/10.1016/j.molliq.2021.116669.
[48] N. Nkosi, K. Tumba, S. Ramsuroop, Measurements of activity coefficient at infinite dilution for organic solutes in tetramethylammonium chloride + ethylene glycol deep eutectic solvent using gas-liquid chromatography, Fluid Phase Equilib. 462 (2018) 31–37, https://doi.org/10.1016/j.fluid.2018.01.019.
[49] L.V.T.D. Alencar, S.B. Rodriguez-Reartes, F.W. Tavares, F. Llovell, A consistent framework to characterize the impact of co-solvents in the key process thermophysical properties of choline chloride-based DESs, J. Ind. Eng. Chem. (2023), https://doi.org/10.1016/j.jiec.2023.11.021.
[50] J.O. Lloret, L.F. Vega, F. Llovell, Accurate description of thermophysical properties of Tetraalkylammonium Chloride Deep Eutectic Solvents with the soft-SAFT equation of state, Fluid Phase Equilib. 448 (2017) 81–93, https://doi.org/10.1016/j.fluid.2017.04.013.
[51] E.A. Crespo, L.P. Silva, J.O. Lloret, P.J. Carvalho, L.F. Vega, F. Llovell, J.A. P. Coutinho, A methodology to parameterize SAFT-type equations of state for solid precursors of deep eutectic solvents: the example of cholinium chloride, PCCP 21 (2019) 15046–15061, https://doi.org/10.1039/C9CP02548K.
[52] N. Pedrosa, J.C. Pàmies, J.A.P. Coutinho, I.M. Marrucho, L.F. Vega, Phase Equilibria of Ethylene Glycol Oligomers and Their Mixtures, Ind. Eng. Chem. Res. 44 (2005) 7027–7037, https://doi.org/10.1021/ie050361t.
[53] L.F. Vega, F. Llovell, F.J. Blas, Capturing the Solubility Minima of n-Alkanes in Water by Soft-SAFT, J. Phys. Chem. B 113 (2009) 7621–7630, https://doi.org/10.1021/jp9018876.
[54] S. Asensio-Delgado, D. Jovell, G. Zarca, A. Urtiaga, F. Llovell, Thermodynamic and process modeling of the recovery of R410A compounds with ionic liquids, Int. J. Refrig 118 (2020) 365–375, https://doi.org/10.1016/j.ijrefrig.2020.04.013.
[55] R. Haghbakhsh, S. Raeissi, Densities and volumetric properties of (choline chloride + urea) deep eutectic solvent and methanol mixtures in the temperature range of 293.15–323.15 K, J. Chem. Thermodyn. (2018) 10–20, https://doi.org/10.1016/j.jct.2018.04.010.
[56] J. Baz, C. Held, J. Pleiss, N. Hansen, Thermophysical properties of glyceline–water mixtures investigated by molecular modelling, PCCP 21 (2019) 6467–6476, https://doi.org/10.1039/C9CP00036D.
[57] A. Yadav, S. Trivedi, R. Rai, S. Pandey, Densities and dynamic viscosities of (choline chloride+glycerol) deep eutectic solvent and its aqueous mixtures in the temperature range (283.15–363.15)K, Fluid Phase Equilib. (2014) 135–142, https://doi.org/10.1016/j.fluid.2014.01.028.
[58] C. Florindo, F.S. Oliveira, L.P.N. Rebelo, A.M. Fernandes, I.M. Marrucho, Insights into the Synthesis and Properties of Deep Eutectic Solvents Based on Cholinium Chloride and Carboxylic Acids, ACS Sustain. Chem. Eng. 2 (2014) 2416–2425, https://doi.org/10.1021/sc500439w.
[59] A. Yadav, S. Pandey, Densities and Viscosities of (Choline Chloride + Urea) Deep Eutectic Solvent and Its Aqueous Mixtures in the Temperature Range 293.15 K to 363.15 K, J. Chem. Eng. Data 59 (2014) 2221–2229, https://doi.org/10.1021/je5001796.
[60] F.S. Mjalli, J. Naser, Viscosity model for choline chloride-based deep eutectic solvents, Asia Pac. J. Chem. Eng. 10 (2015) 273–281, https://doi.org/10.1002/apj.1873.
[61] R. Ramezani, S. Mazinani, R. Di Felice, Characterization and kinetics of CO2 absorption in potassium carbonate solution promoted by 2-methylpiperazine, Journal of Environmental, Chem. Eng. 6 (2018) 3262–3272, https://doi.org/10.1016/j.jece.2018.05.019.
[62] S. Sarmad, Y. Xie, J.-P. Mikkola, X. Ji, Screening of deep eutectic solvents (DESs) as green CO2 sorbents: from solubility to viscosity, New J. Chem. 41 (2017) 290–301, https://doi.org/10.1039/C6NJ03140D.
[63] E. Cané, F. Llovell, L.F. Vega, Accurate viscosity predictions of linear polymers from n-alkanes data, J. Mol. Liq. 243 (2017) 115–123, https://doi.org/10.1016/j.molliq.2017.08.033.
[64] M.B. Oliveira, S.V.D. Freitas, F. Llovell, L.F. Vega, J.A.P. Coutinho, Development of simple and transferable molecular models for biodiesel production with the soft-SAFT equation of state, Chem. Eng. Res. Des. 92 (2014) 2898–2911, https://doi.org/10.1016/j.cherd.2014.02.025.
[65] R. Tillner-Roth, H.D. Baehr, An International Standard Formulation for the Thermodynamic Properties of 1,1,1,2-Tetrafluoroethane (HFC-134a) for Temperatures from 170 K to 455 K and Pressures up to 70 MPa, J. Phys. Chem. Ref. Data 23 (1994) 657–729, https://doi.org/10.1063/1.555958.
[66] P.J. Castro, A.E. Redondo, J.E. Sosa, M.E. Zakrzewska, A.V.M. Nunes, J.M. M. Araújo, A.B. Pereiro, Absorption of Fluorinated Greenhouse Gases in Deep Eutectic Solvents, Ind. Eng. Chem. Res. 59 (2020) 13246–13259, https://doi.org/10.1021/acs.iecr.0c01893.
[67] W.A. Fouad, L.F. Vega, Next Generation of Low Global Warming Potential Refrigerants: Thermodynamic Properties Molecular Modeling 64 (2018) 250–262, https://doi.org/10.1002/aic.15859.
[68] C. Cadena, J.L. Anthony, J.K. Shah, T.I. Morrow, J.F. Brennecke, E.J. Maginn, Why Is CO2 So Soluble in Imidazolium-Based Ionic Liquids? J. Am. Chem. Soc. 126 (2004) 5300–5308, https://doi.org/10.1021/ja039615x.
[69] F. Llovell, M.B. Oliveira, J.A.P. Coutinho, L.F. Vega, Solubility of greenhouse and acid gases on the [C4mim][MeSO4] ionic liquid for gas separation and CO2 conversion, Catal. Today 255 (2015) 87–96, https://doi.org/10.1016/j.cattod.2014.12.049.
[70] R. Sander, W.E. Acree, A.D. Visscher, S.E. Schwartz, T.J. Wallington, Henry's Law Constants (IUPAC Recommendations 94 (2022) (2021) 71–85.
[71] A. Mejía, E.A. Müller, G. Chaparro Maldonado, SGTPy: A Python Code for Calculating the Interfacial Properties of Fluids Based on the Square Gradient Theory Using the SAFT-VR Mie Equation of State, Journal of Chemical Information and Modeling, 61 (2021) 1244-1250. doi: 10.1021/acs.jcim.0c01324.
[72] W. Chen, Z. Xue, J. Wang, J. Jiang, X. Zhao, T. Mu, Investigation on the Thermal Stability of Deep Eutectic Solvents, Acta Phys. -Chim. Sin. 34 (2018) 904–911, https://doi.org/10.3866/pku.Whxb201712281.
[73] S. Liu, D. Yu, Y. Chen, R. Shi, F. Zhou, T. Mu, High-Resolution Thermogravimetric Analysis Is Required for Evaluating the Thermal Stability of Deep Eutectic Solvents, Ind. Eng. Chem. Res. 61 (2022) 14347–14354, https://doi.org/10.1021/acs.iecr.2c02240.
[74] Y. Chen, D. Yu, Y. Lu, G. Li, L. Fu, T. Mu, Volatility of Deep Eutectic Solvent Choline Chloride:N-Methylacetamide at Ambient Temperature and Pressure, Ind. Eng. Chem. Res. 58 (2019) 7308–7317, https://doi.org/10.1021/acs.iecr.8b04723.
[75] D. Jovell, J.O. Pou, F. Llovell, R. Gonzalez-Olmos, Life Cycle Assessment of the Separation and Recycling of Fluorinated Gases Using Ionic Liquids in a Circular Economy Framework, ACS Sustain. Chem. Eng. 10 (2022) 71–80, https://doi.org/10.1021/acssuschemeng.1c04723.